
Mass-loss rates from sub-millimetre and radio data

Ronny Blomme



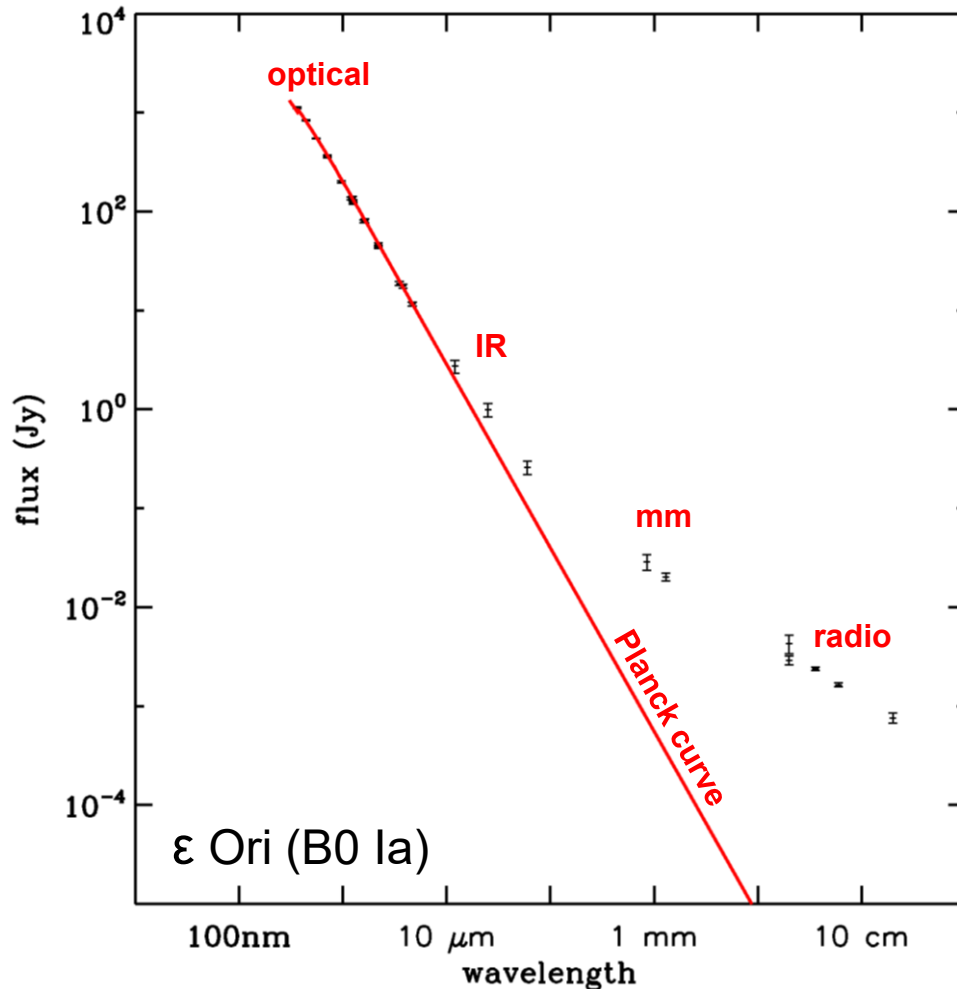
Overview

- A simple model
- Complications due to clumping/porosity
- More complications due to binaries
- And more complications due to magnetic fields
- Resolving the stellar wind
- Upgraded and new instrumentation

Radio emission from massive stars

The observed radio flux is much higher than expected from a Planck curve.

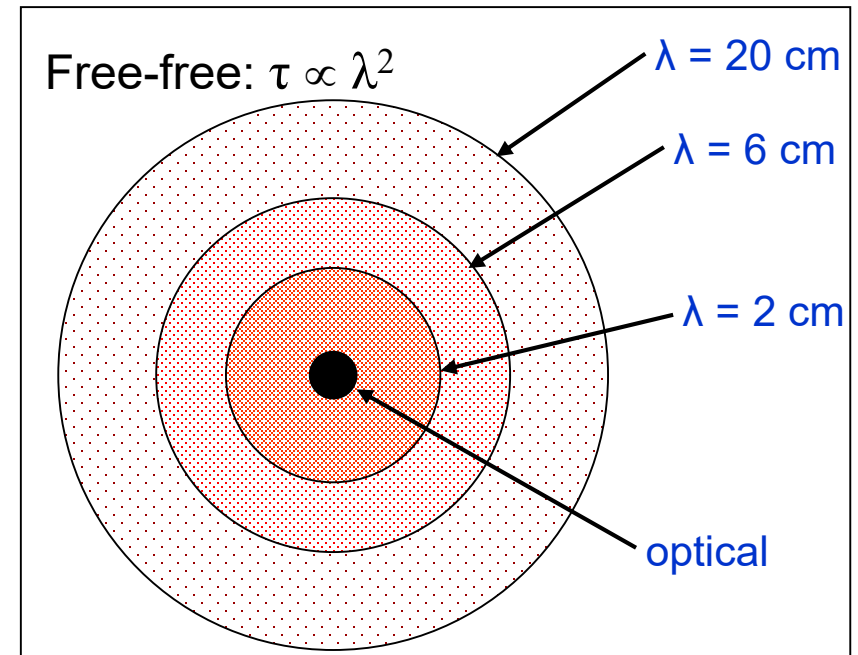
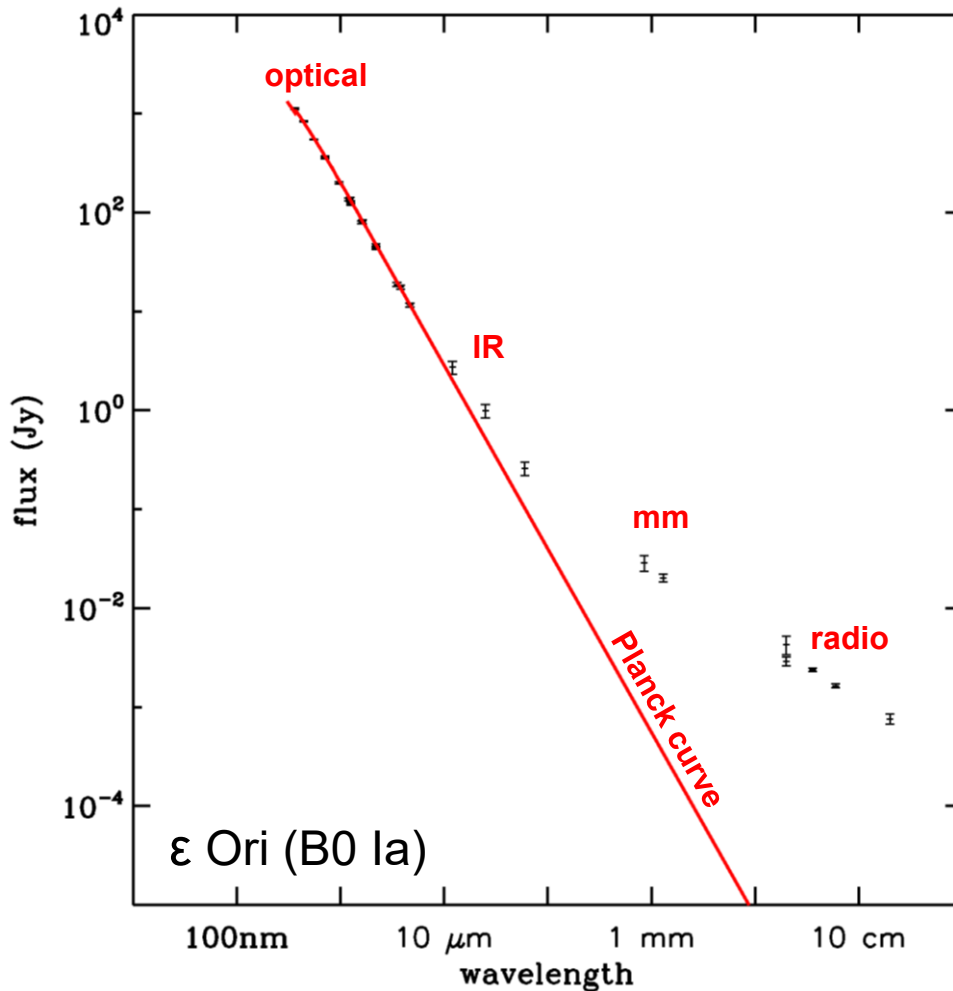
This is due to free-free processes in the ionized material of the stellar wind.



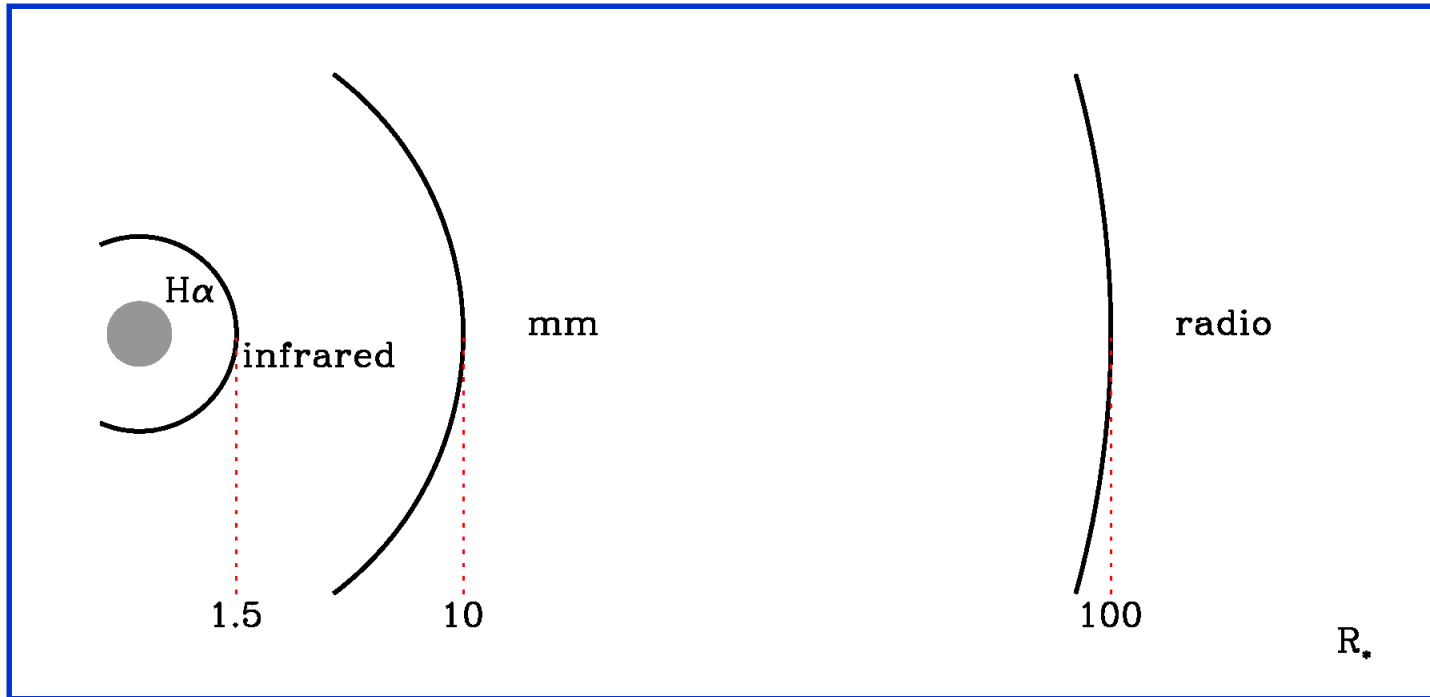
1 mJy = $10^{-29} \text{ W m}^{-2} \text{ Hz}^{-1}$
= $10^{-26} \text{ erg s}^{-1} \text{ cm}^{-2} \text{ Hz}^{-1}$

Radio emission

Because of the λ^2 dependence of the free-free process, the star seems larger at longer wavelengths.



Formation regions



A simple model (Wright & Barlow, 1975)

Wright and Barlow solved the radiative transfer equation through the wind, and determined the emergent flux.

■ Assumptions

- Time-independent
- Spherical symmetry
- Constant velocity
- Constant temperature
- Only free-free process
- No electron scattering
- No Doppler shifts (continuum)
- H+He only, fully ionized
- Neglect the presence of the star

A simple model (Wright & Barlow, 1975)

See Wright and Barlow paper for the appropriate units of all quantities in the equation.

- Resulting flux:

$$F_\nu = 23.2 \left(\frac{\dot{M}}{\mu v_\infty} \right)^{4/3} \frac{\nu^{2/3}}{D^2} \left(\gamma g_{\text{ff}} \overline{Z^2} \right)^{2/3}$$

See Wright and Barlow paper for the appropriate units of all quantities in the equation.

A simple model (Wright & Barlow, 1975)

- Resulting flux:

$$F_\nu = 23.2 \left(\frac{\dot{M}}{\mu v_\infty} \right)^{4/3} \frac{\nu^{2/3}}{D^2} \left(\gamma g_{\text{ff}} \bar{Z}^2 \right)^{2/3}$$

Diagram illustrating the equation for flux F_ν with labels for variables:

- mass-loss rate (points to \dot{M})
- frequency (points to ν)
- terminal velocity (points to v_∞)
- distance (points to D)

$$F_\nu \propto \nu^\alpha \propto \lambda^{-\alpha} \quad \alpha = +0.6 \text{ spectral index}$$

MASS-LOSS RATES FROM RADIO OBSERVATIONS

Bieging et al. 1989

STAR (1)	SPECTRAL TYPE (2)	S_{ν} (mJy)		g_{ff}		V_{∞} (km s ⁻¹)	μ (8)	DISTANCE (kpc) (9)	$\log \dot{M}$ (M_{\odot} yr ⁻¹)		
		$\lambda 2$ cm (3)	$\lambda 6$ cm (4)	$\lambda 2$ cm (5)	$\lambda 6$ cm (6)				free-free (10)	Theoretical (11)	Empirical (12)
Definite Free-Free Sources											
ζ Pup	O4f	3.0	1.3	5.1	5.7	2400	1.5	0.45	-5.3	-5.4	-5.4
HD 152408	O8 Ifp	2.4	1.1	4.9	5.5	1800	1.3	1.90	-4.6	-5.2	-5.3
ζ^1 Sco	B1 Ia ⁺	4.3	1.7	4.5	5.1	500	1.4	1.90	-5.0	-4.1	-4.9
HD 169454	B1 Ia	1.9	1.0	4.5	5.1	850 ^a	1.3	1.66	-5.1	-4.5	-5.3
P Cyg	B1 Ia ⁺	...	6.4v ^b	...	5.1	220	1.4	1.82	-5.0v	-4.3	-5.1
Cyg OB2 No. 12	B8 Ia	...	2.9v ^c	...	4.6	(1400)	1.4	1.82	(-4.4v)	-4.1	-4.9
Probable Free-Free Sources											
HD 15570	O4f	...	≤0.2	...	5.7	2700	1.3	2.19	≤-5.0	-4.7	-4.5
HD 166734	O7.5f + O9	...	0.4	...	5.6	2600	1.5	(2.40)	-4.6	-4.6	-4.7
HD 151804	O8 If	...	0.4	...	5.5	2000	1.3	1.90	-5.0	-5.0	-5.1
α Cam	O9.5 Ia	...	0.4	...	5.4	1800	1.5	(1.1)	-5.3	-5.5	-5.6

Abbott et al. 1986

DERIVED STELLAR WIND PARAMETERS

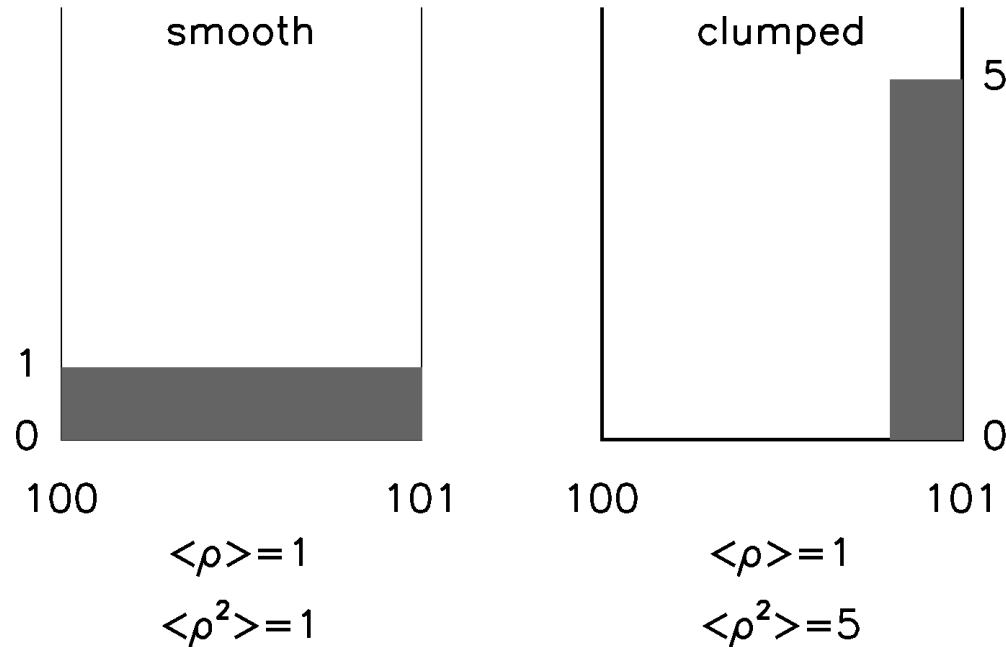
W-R	Spectral Type	V_{∞} (km s ⁻¹)	Source ^a of V_{∞} (Ref.)	C_5 ^b	$\log \dot{M}$ (M_{\odot} yr ⁻¹)	$\sigma(\log \dot{M})$ ^c	$\dot{M} V_{\infty}$ (10 ²⁹ gm cm s ⁻¹)	$\frac{1}{2} \dot{M} V_{\infty}^2$ (10 ³⁷ ergs s ⁻¹)
Thermal Wind Radio Sources								
142	W02	7400±900	(9)	0.8×10 ⁻⁶	<-4.7	0.2	(9.3)	(34.0)
111	WC5	3550±150	(10)	0.8	-4.8	0.2	3.3	5.9
114	WC5	2600±350	(9)	0.8	<-4.8	0.2	(2.5)	(3.2)
143	WC5	4000±600	(9)	0.8	<-5.1	0.3	(1.9)	(3.8)
93	WC7+Abs	3100±200	(9)	0.9	-4.5	0.3	6.2	9.6

The radio region is probably the best spectral domain for determining accurate mass loss rates for individual stars. Once the radio flux at a given frequency has been measured, only the terminal velocity of the wind (obtainable from ultraviolet spectra) and the distance of the star are required in order to obtain the mass loss rate.

Barlow 1979

One complication for this simple model is presence of clumping.

Clumping



Clumping factor: $f_{cl} = \langle \rho^2 \rangle / \langle \rho \rangle^2$

Volume filling factor = $1/f_{cl}$, in this simple approximation

Effect of clumping on radio flux

$$F_\nu = 23.2 \left(\frac{\dot{M} \sqrt{f_{cl}}}{\mu v_\infty} \right)^{4/3} \frac{\nu^{2/3}}{D^2} \left(\gamma g_{ff} \overline{Z^2} \right)^{2/3}$$

- Two interpretations:
 - Clumping => higher flux
 - Given flux: lower mass-loss rate, higher clumping factor

- Degeneracy mass-loss rate and clumping factor

Clumping

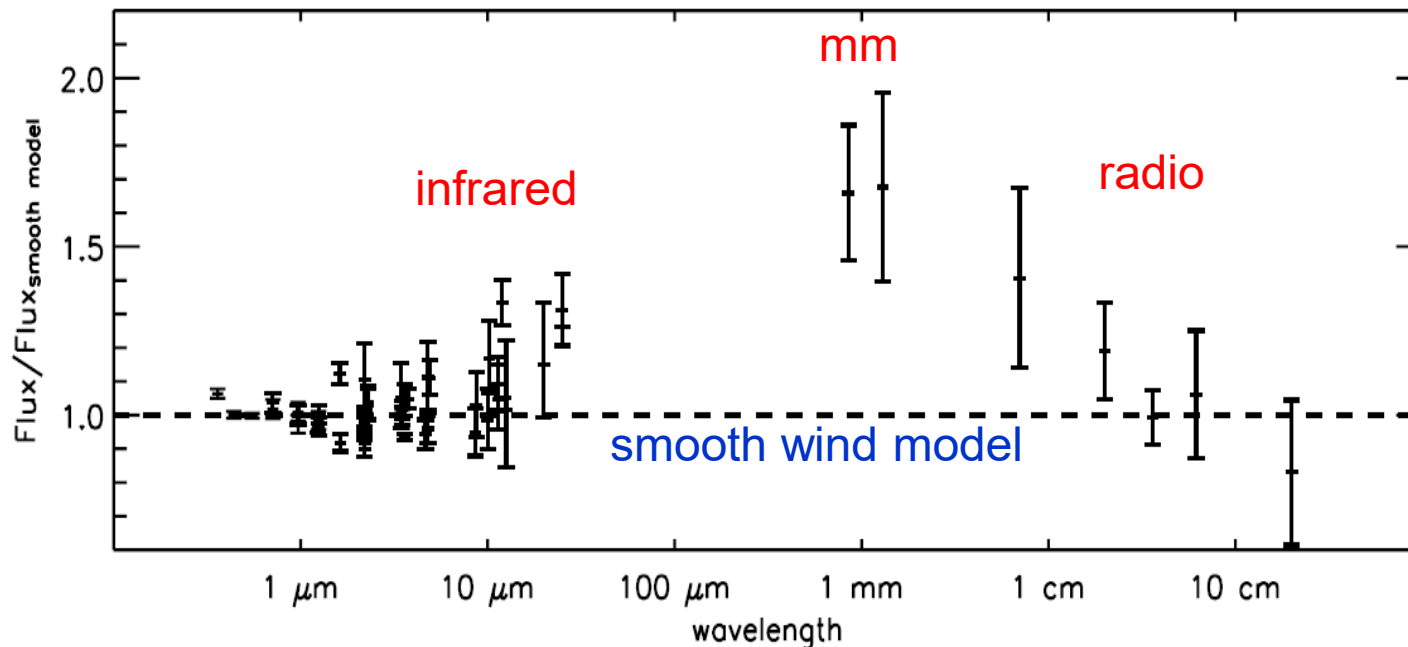
ϵ Ori = HD 37128 (B0 Ia)

- Fit smooth-wind model to visual+near-infrared and radio observations

A smooth wind cannot explain all mm+radio observations. So, there must be clumping.

But: a single clumping factor cannot explain all mm+radio observations either.

So, clumping factor changes with distance.



Blomme et al. 2002 (+ 20 cm obs)

For this plot, the 3.6 cm flux was assumed to be “clumping free”. But of course, it is unlikely that this would be correct.

Comparison radio – infrared, mm, H α

- Puls et al. 2006
 - 19 O-type supergiants/giants
 - divide wind into 5 regions
 - clumping factor constant in each region
 - adjust clumping factors to fit the observations
 - radio region: assume no clumping

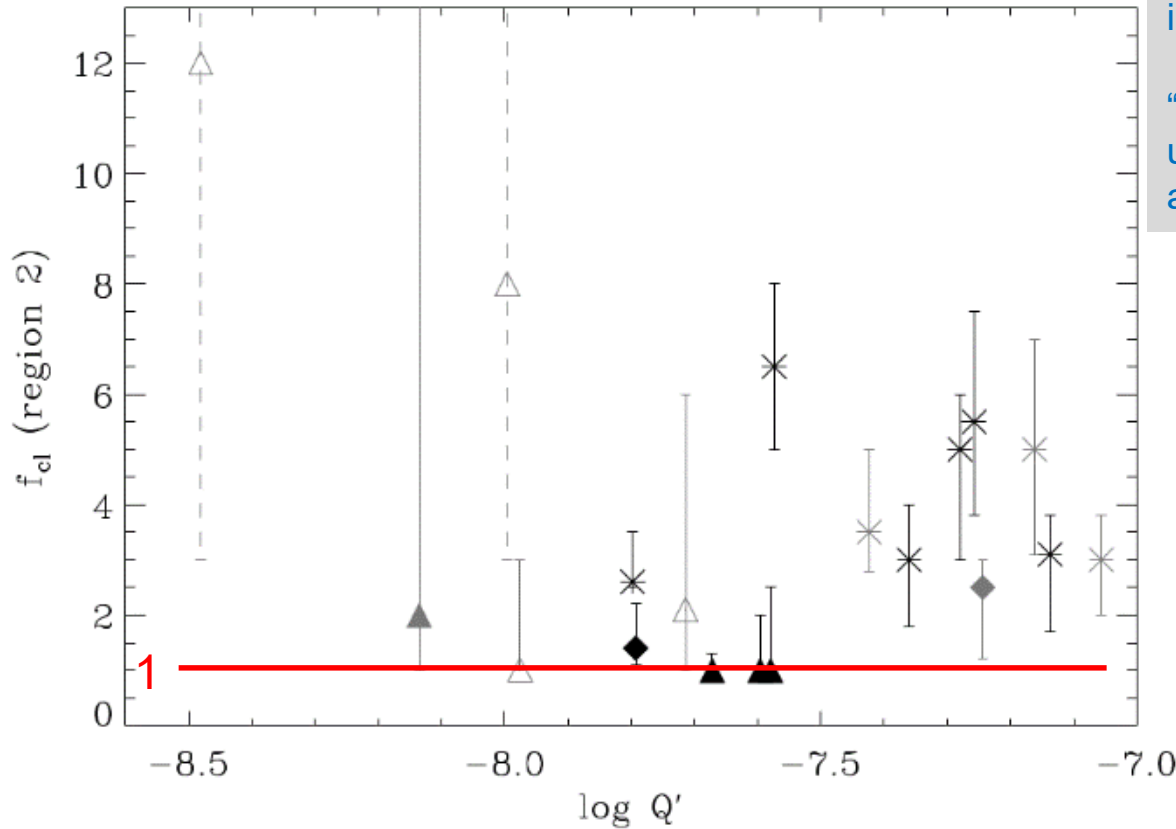
Clumping

Denser winds: innermost region is more strongly clumped than the outermost one.

Thinner winds: similar clumping properties in the inner and outer regions.

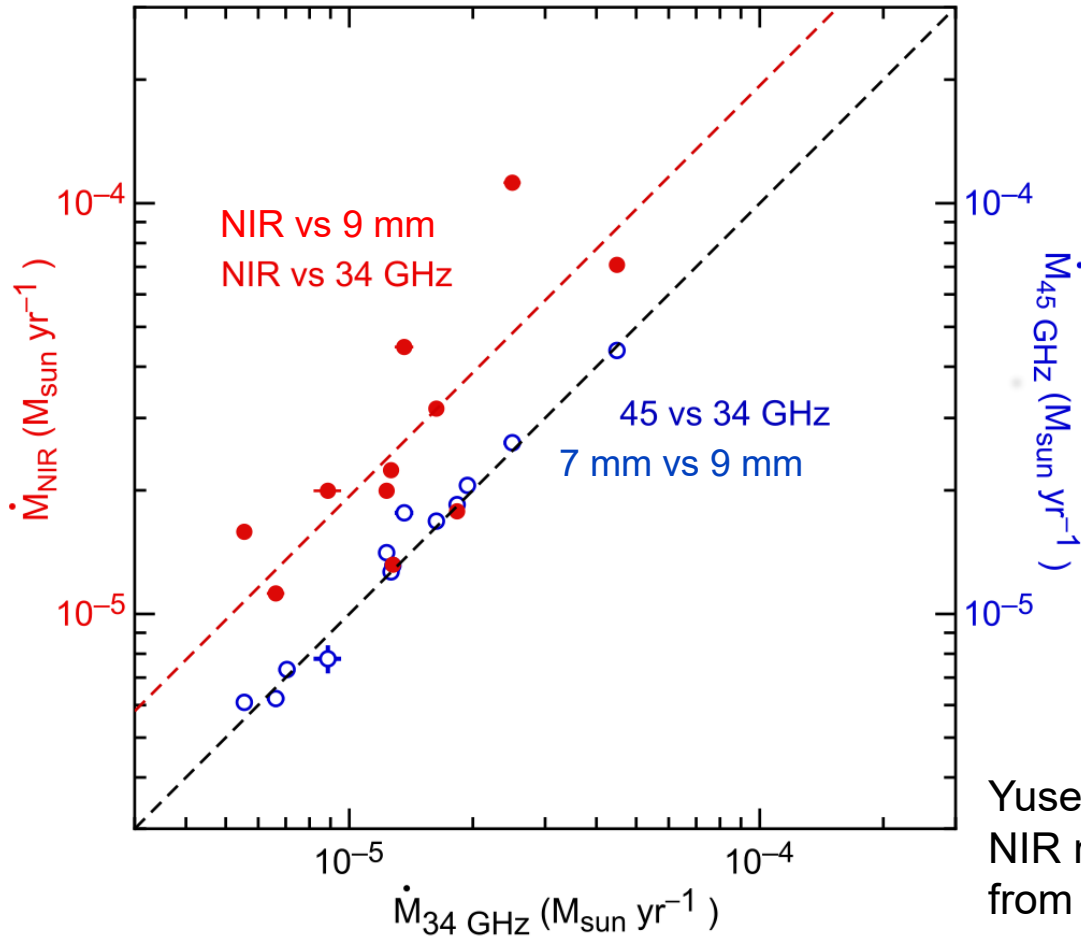
“Absolute” value of the clumping factor is unknown. All we know is that clumping is at minimum in the radio formation region.

clumping factor in H α region



Puls et al. 2006

Clumping



The 7mm and 9mm smooth-wind mass-loss rates agree well.

The near-infrared (NIR) smooth-wind mass-loss rates are on average a factor of 2 higher than the 9 mm ones.

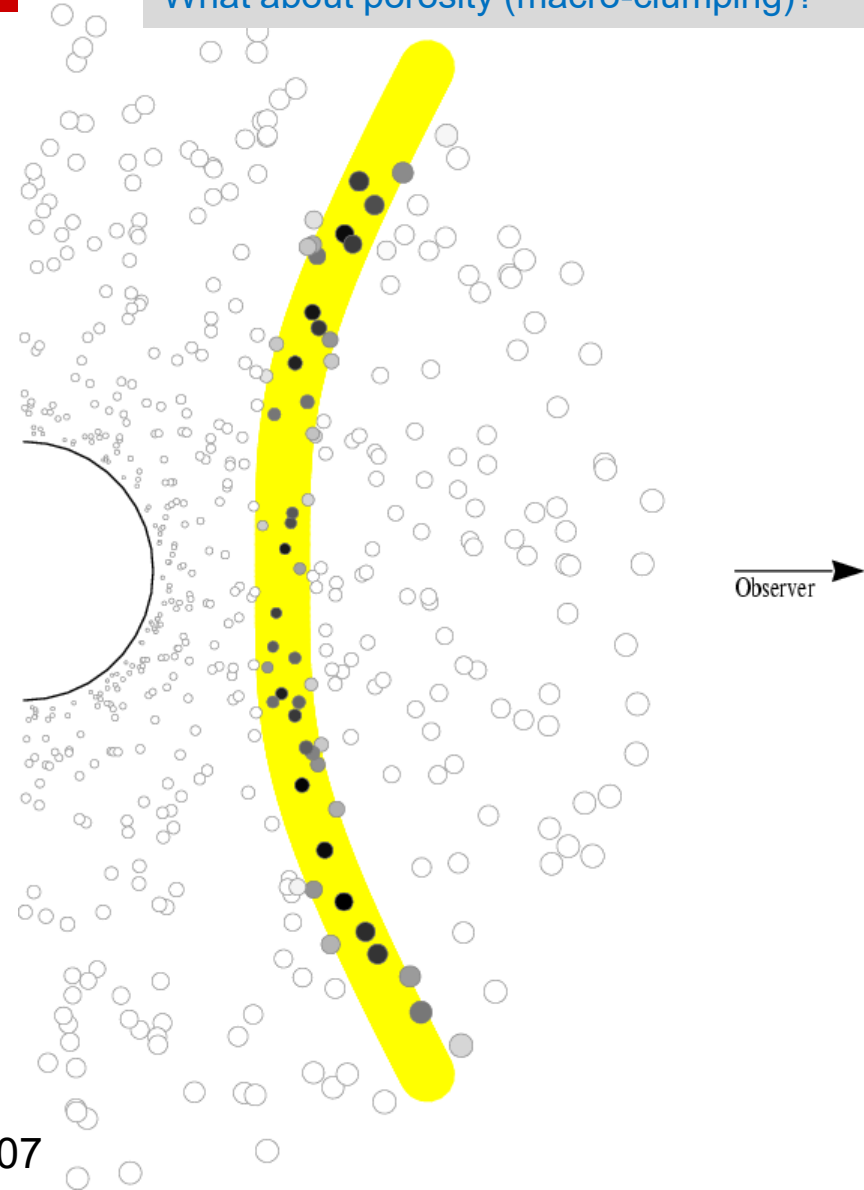
This points to clumping changing with distance in the stellar winds of WR stars.

Yusef-Zadeh et al. 2015
NIR mass-loss rates
from Martins et al. 2007

So far, we considered only optically thin clumping (micro-clumping).
What about porosity (macro-clumping)?

Porosity

- Clumping
 - Clumps are optically thin
 - Micro-clumping
- Porosity
 - Clumps can have any optical thickness
 - Macro-clumping



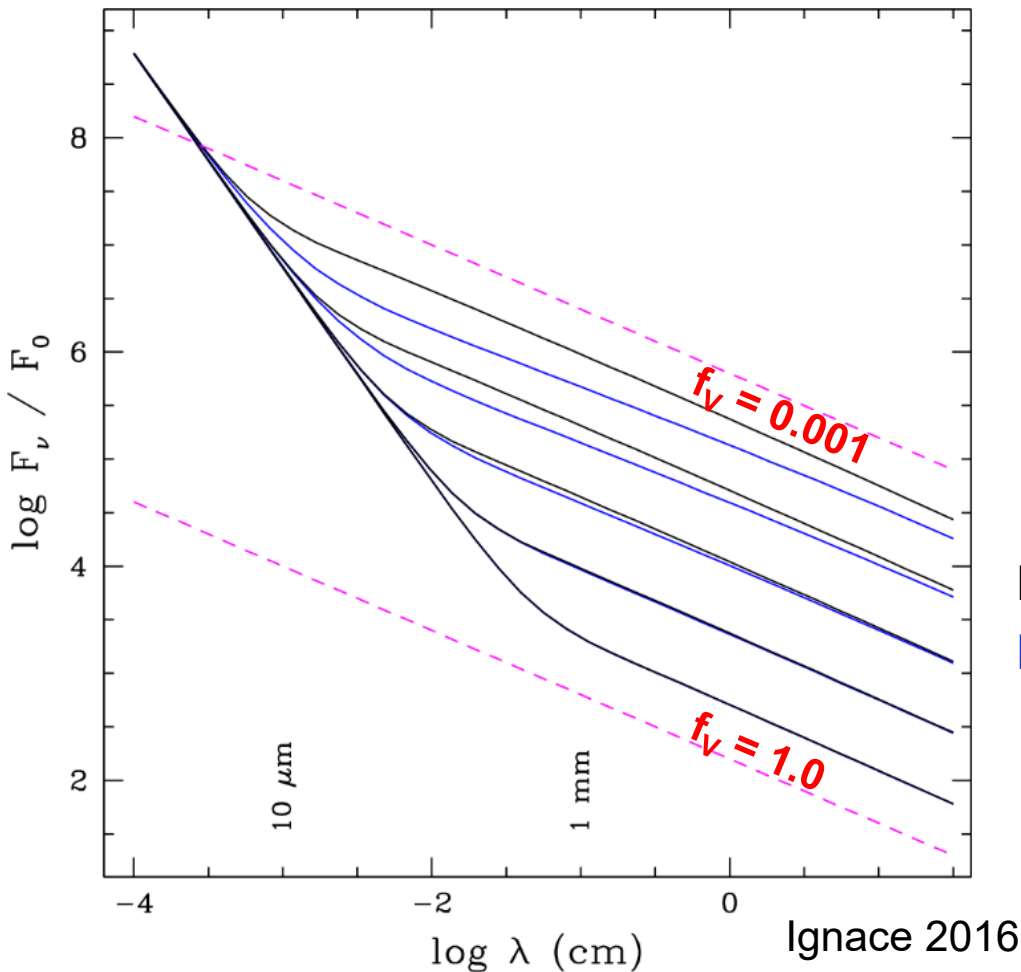
Oskinova et al. 2007

Porosity – flux

Porosity due to spherical clumps, compared to micro-clumping, for a range of volume filling factors.

Very small volume filling factors (large clumping factors) are needed to make a difference.

Even then, there is the degeneracy between mass-loss rate and porosity.



Black line: micro-clumping
Blue line : porosity

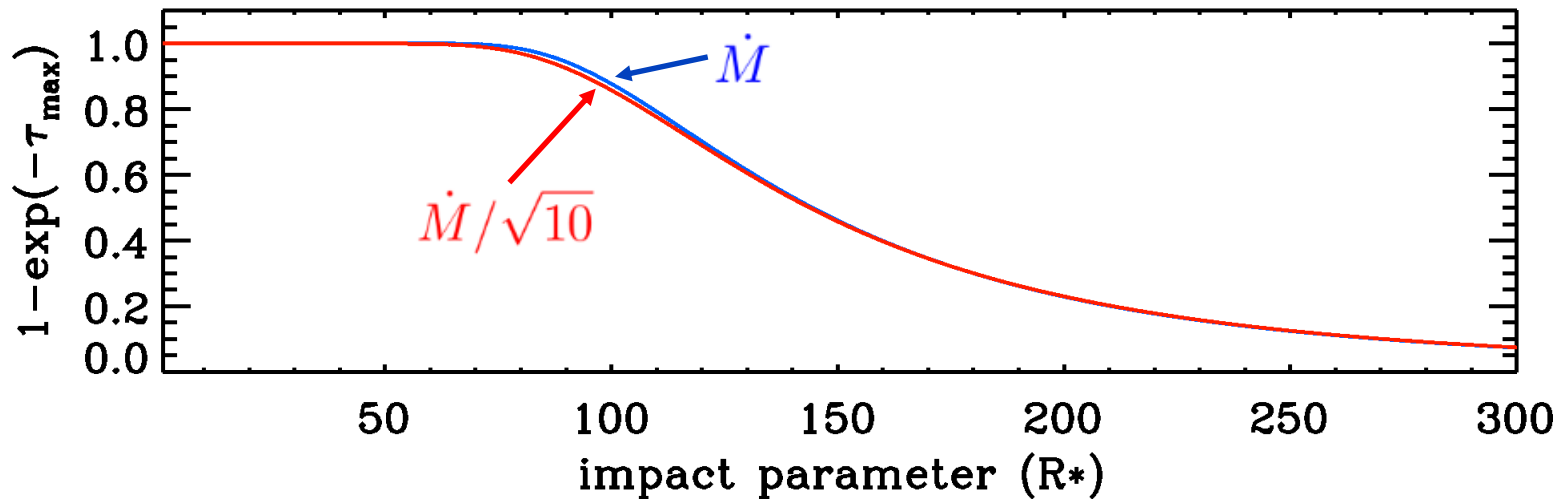
Porosity – optical depth

Comparison between smooth wind with mass-loss rate \dot{M} and porous wind with mass-loss rate $\dot{M}/\sqrt{10}$.

Degeneracy: flux is almost identical.

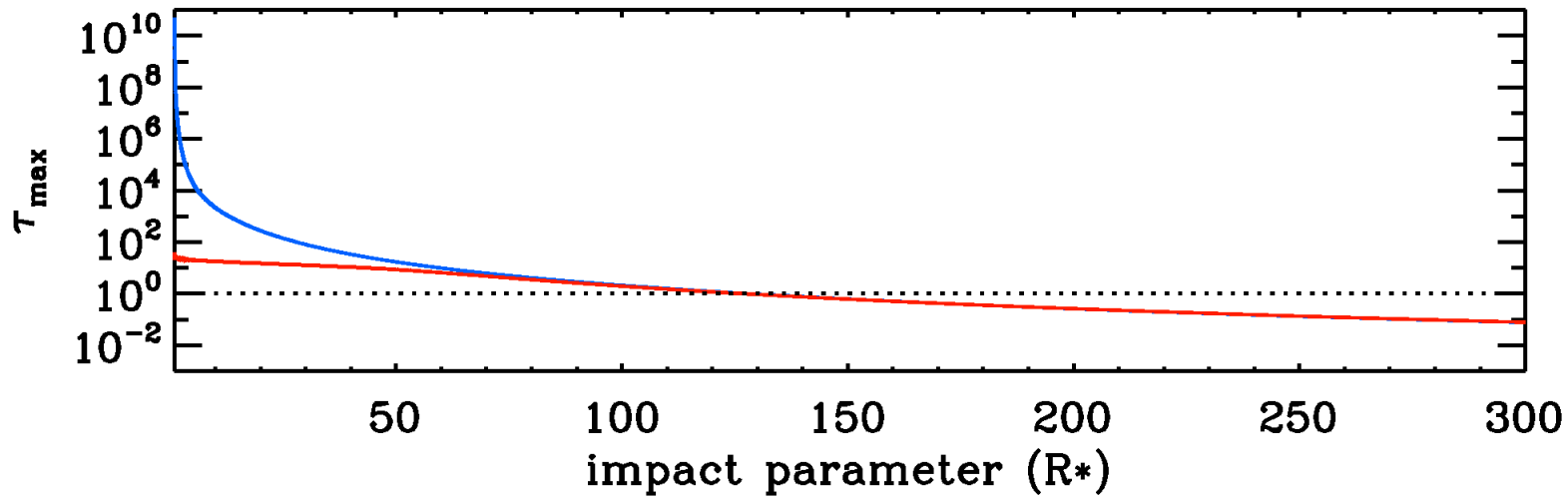
$$F_\nu = \frac{B_\nu(T)}{D^2} \int_0^{+\infty} 2\pi p dp (1 - \exp(-\tau_{\max}(T, p)))$$

$$\tau_{\max}(T, p) = \frac{\pi}{2} K(\nu, T) \bar{Z}^2 \gamma \left(\frac{\dot{M} \sqrt{f_{cl}}}{\mu m_H 4\pi v_\infty} \right)^2 \frac{1}{p^3}$$



Porosity – optical depth

But optical depth is very different. So, you can look deeper into the wind.



$$\frac{L}{R_*} = 0.2 \left[\left(\frac{r}{R_*} \right)^2 \frac{v(r)}{v_\infty} \right]^{1/3}$$

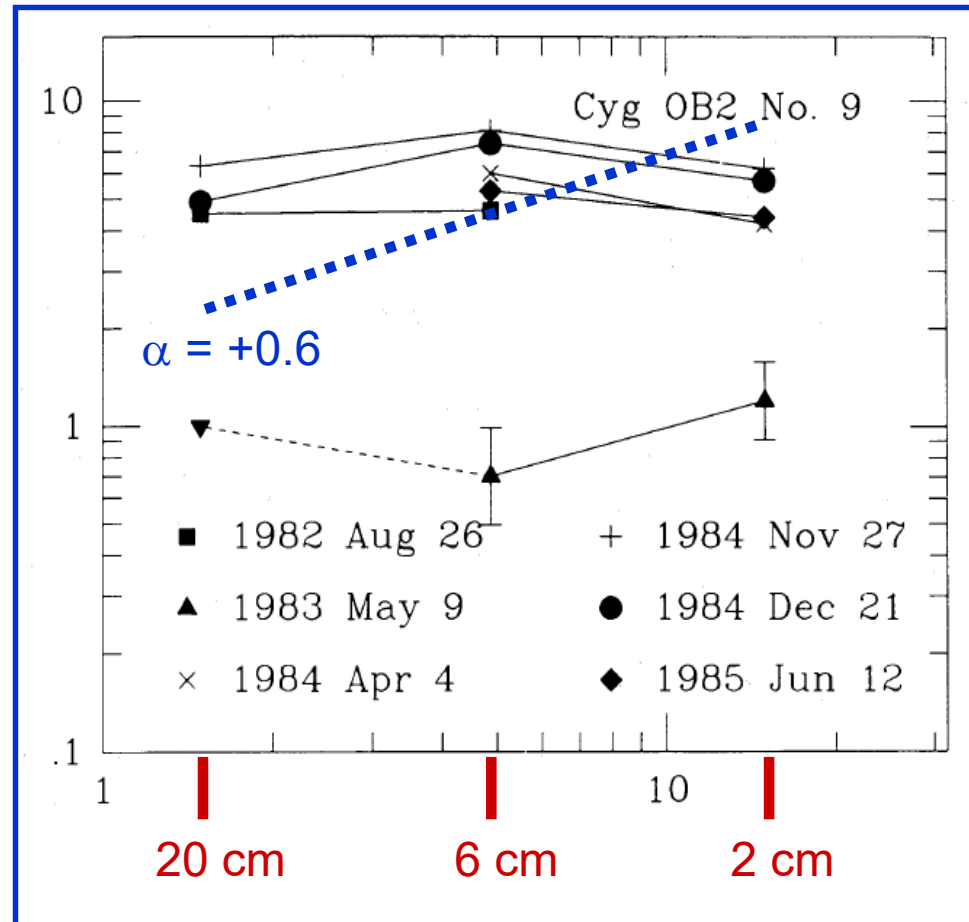
Non-thermal radio emission

Non-thermal radio emission can be recognized in a number of ways.

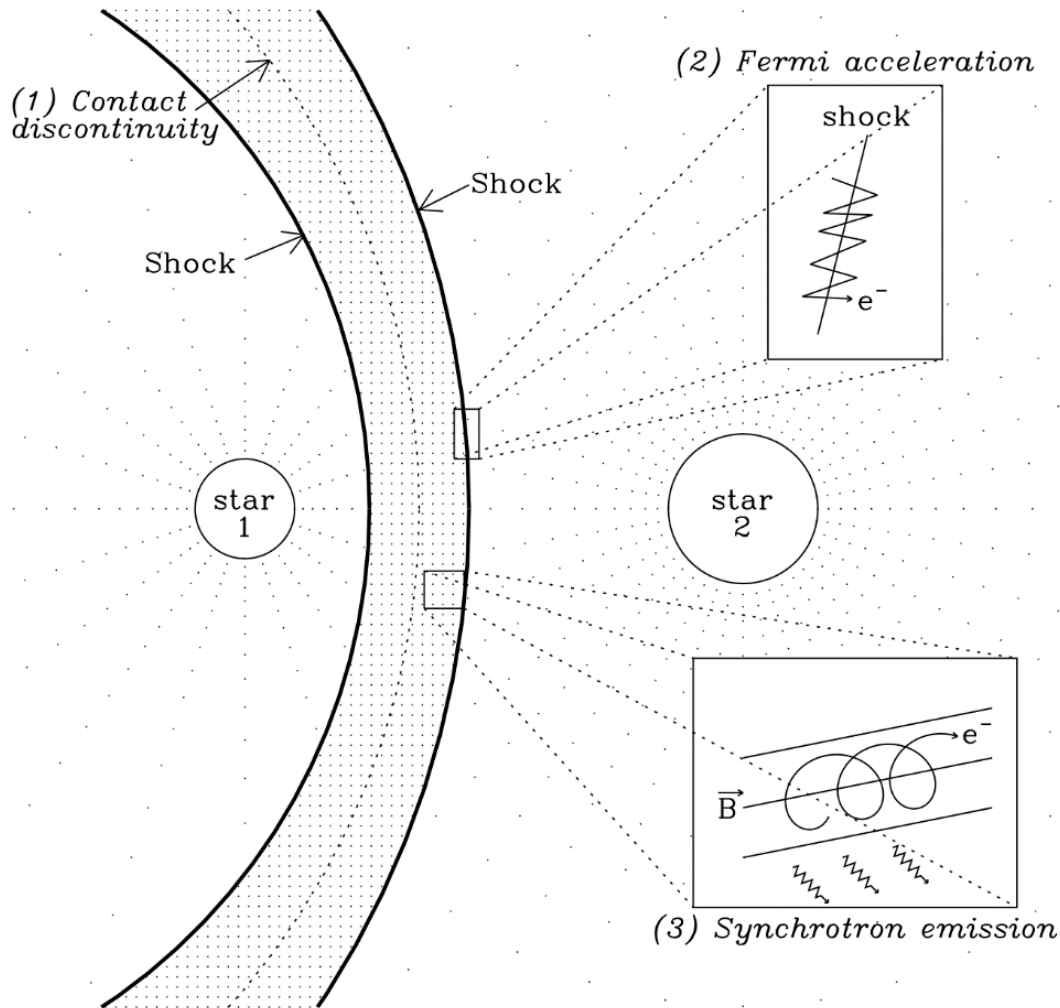
- High flux
- Variability
- Spectral index non-thermal

$$F_\nu \propto \nu^\alpha \propto \lambda^{-\alpha}$$

Bieging et al. 1989



Colliding winds



1. The winds of both components collide, creating a shock on either side of the contact discontinuity.
2. At each shock, the Fermi mechanism accelerates a fraction of the electrons to relativistic speeds.
3. These relativistic electrons spiral in the magnetic field and emit synchrotron radiation.

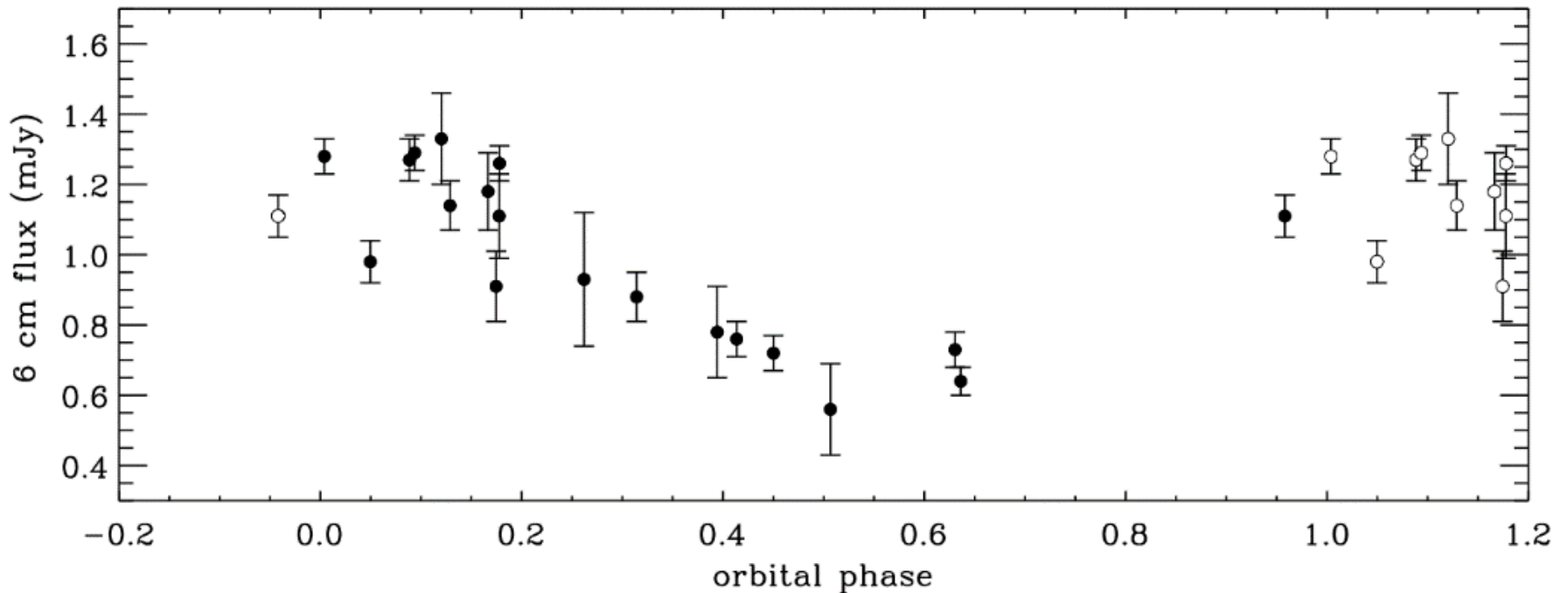
Blomme 2011

Colliding winds in O+O binaries

Non-thermal radio emission from O stars can also be explained by colliding-wind binaries.

This can be seen because the radio fluxes vary consistently with orbital phase (over many orbits).

Cyg OB2 #8A



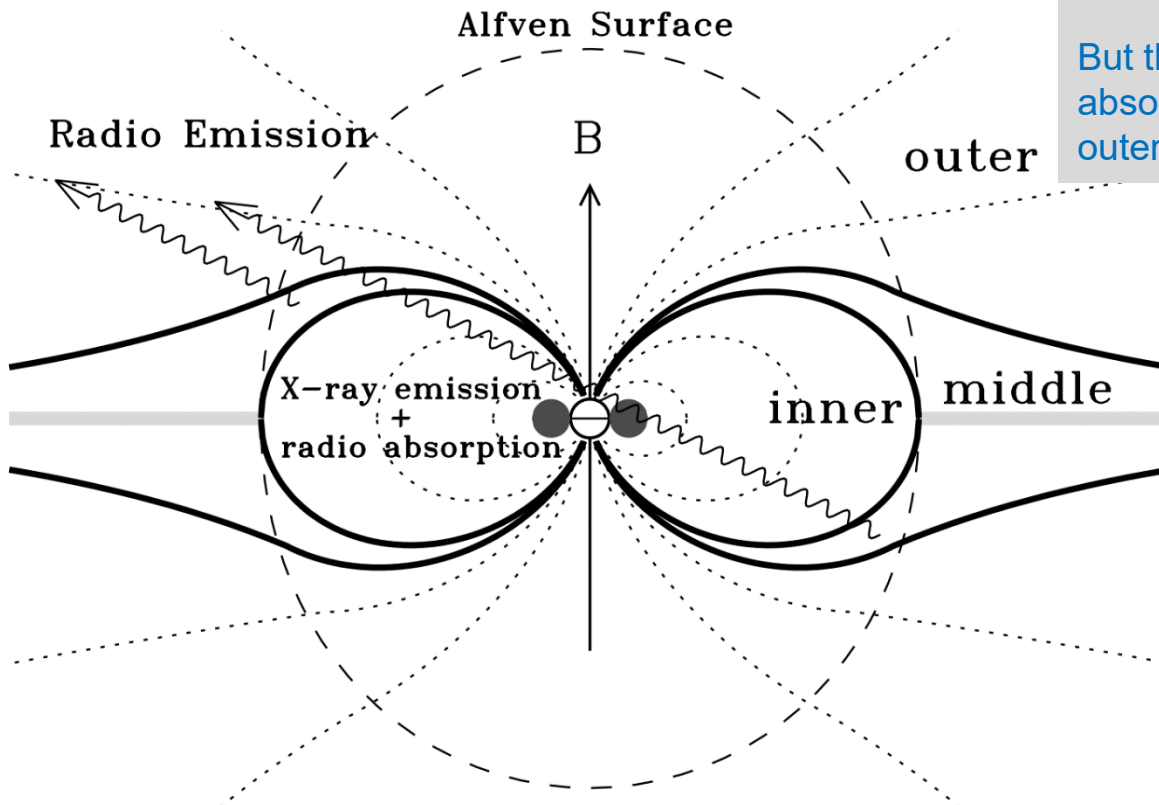
Blomme et al. 2010

Magnetic OB stars

In magnetic stars, electrons can get accelerated at the current sheet, or in shocks in the inner magnetosphere.

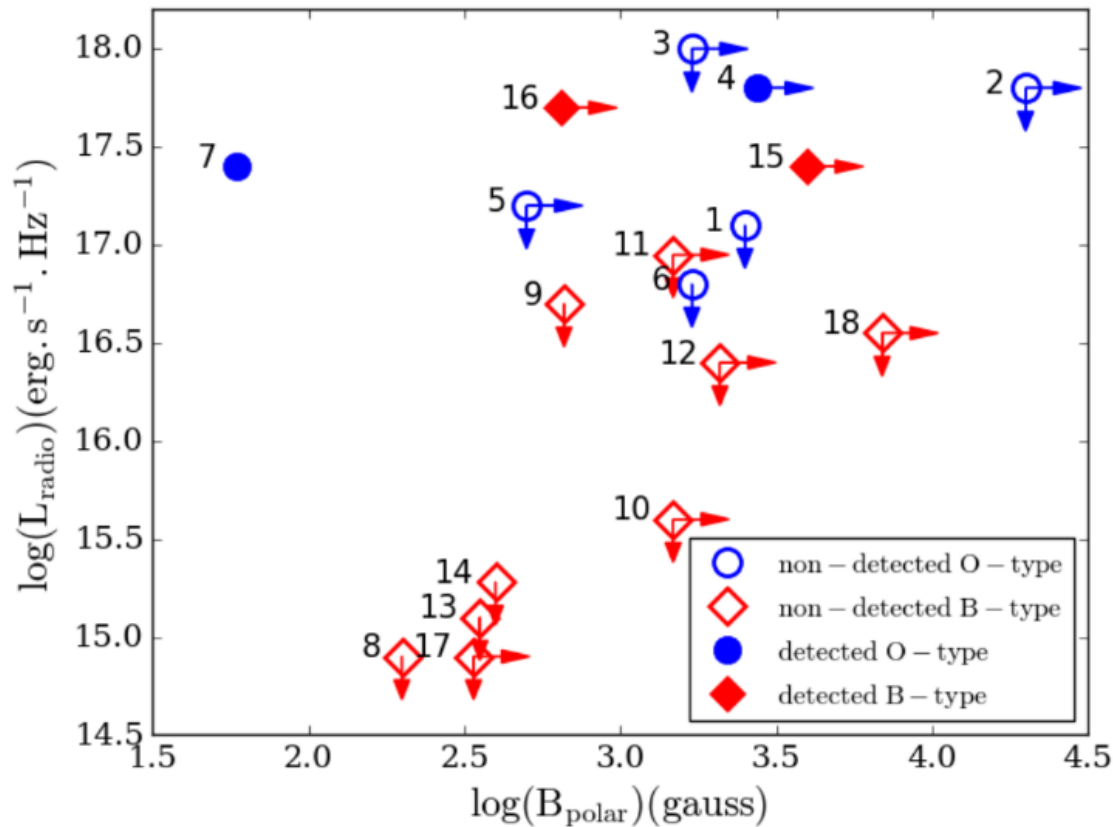
These give rise to gyrosynchrotron radiation.

But this radiation can still be (partly?) absorbed by the free-free absorption in the outer stellar wind.



Trigilio et al. 2004

Magnetic OB stars



2 out of 7 O-type stars detected (both binaries) @ 3 cm.

2 out of 11 B-type stars (not binaries) detected @ 3 cm.

Fluxes are much too high for 3 of these 4 stars, assuming thermal free-free emission only.

For the detected B-type stars, this could indicate the effect of a magnetosphere on the radio fluxes.

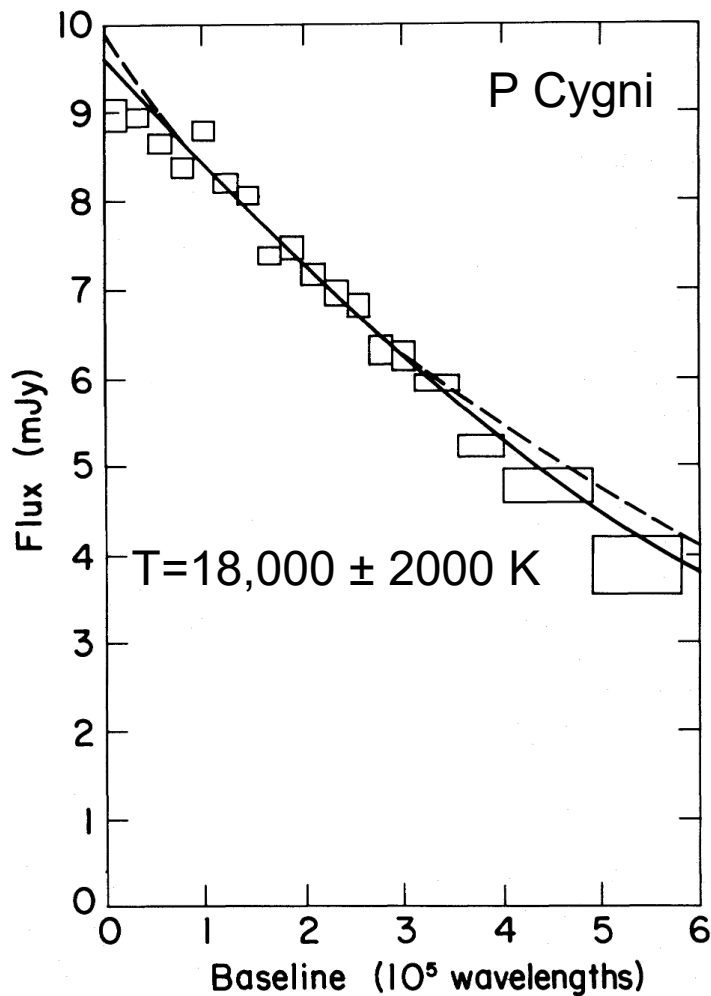
Kurapati et al. 2017

Resolved stellar winds

Plotting the visibilities as a function of baseline.

The visibilities are the Fourier-transform of the brightness on the sky.

By fitting the visibilities of a resolved stellar wind, you can determine the temperature in the wind.



White and Becker (1982)

Resolved clumping/porosity?

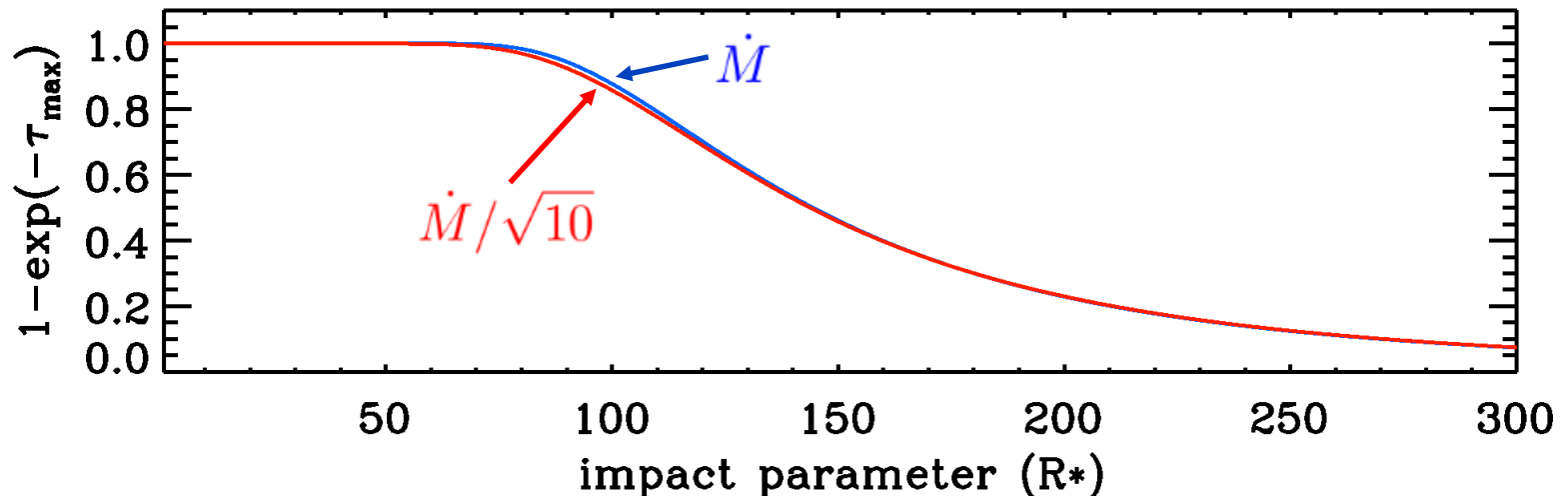
Can we derive information about clumping/porosity from resolving the wind?

No, because of the degeneracy between mass-loss rate and the clumping/porosity parameters.

This degeneracy is best seen in the $1 - \exp(-\tau_{\max})$ function, which determines mainly the brightness distribution on the sky.

$$F_{\nu} = \frac{B_{\nu}(T)}{D^2} \int_0^{+\infty} 2\pi p dp (1 - \exp(-\tau_{\max}(T, p)))$$

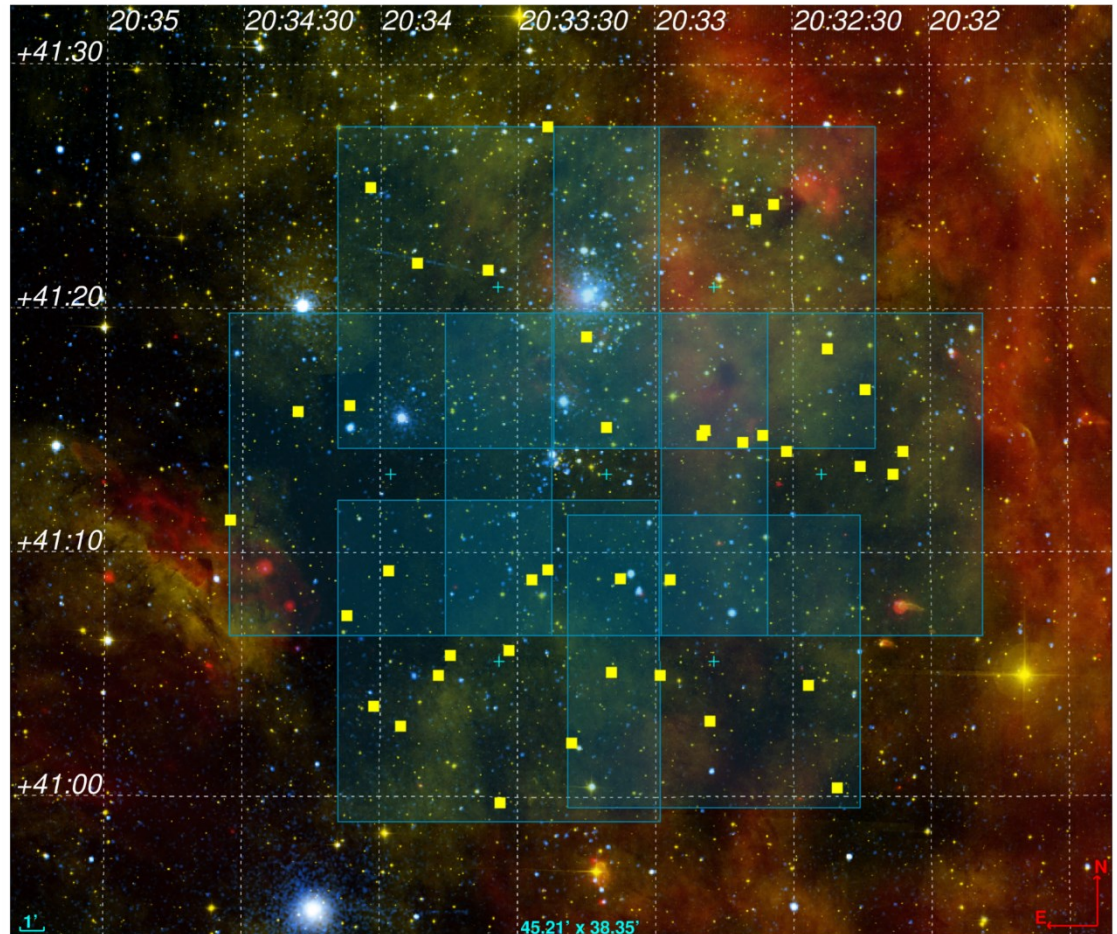
$$\tau_{\max}(T, p) = \frac{\pi}{2} K(\nu, T) \bar{Z}^2 \gamma \left(\frac{\dot{M} \sqrt{f_{cl}}}{\mu m_H 4\pi v_{\infty}} \right)^2 \frac{1}{p^3}$$



e-MERLIN

Fields observed at 20 cm in the
Cyg OB2 region for COBRaS.

COBRaS Legacy Project
Cyg OB2 Radio Survey
PI: Raman Prinja



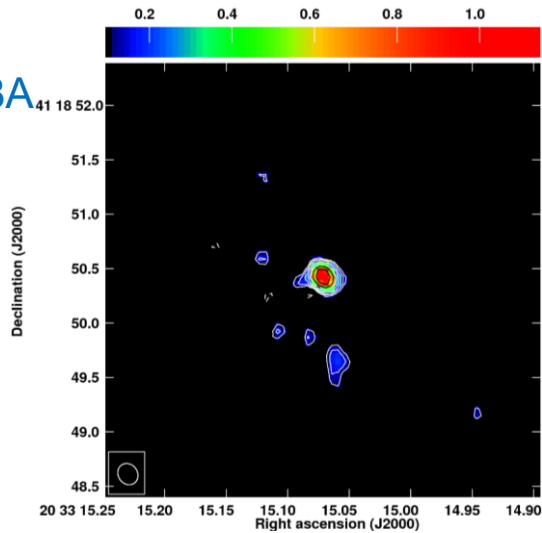
Morford et al. 2017, submitted

Upgraded and new interferometers

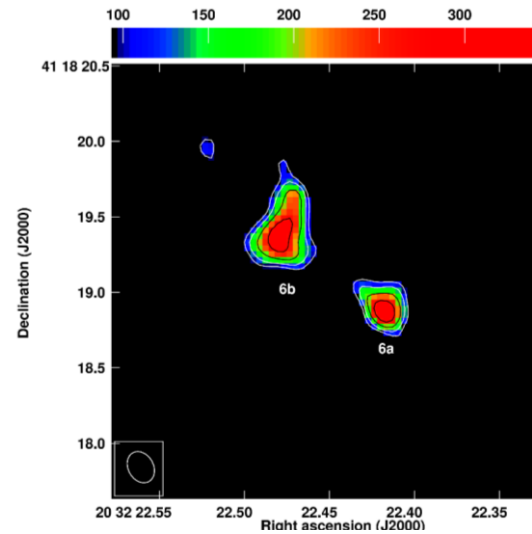
A major advantage of recent upgrades is that a wide field can now be accurately imaged. This is useful in studying clusters.

e-MERLIN - COBRaS

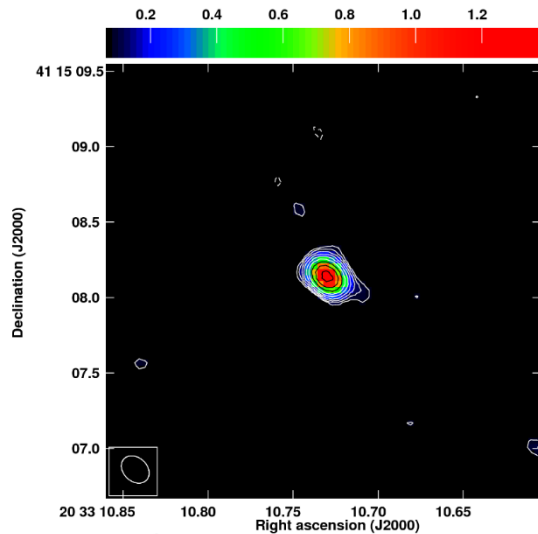
Cyg OB2 #8A



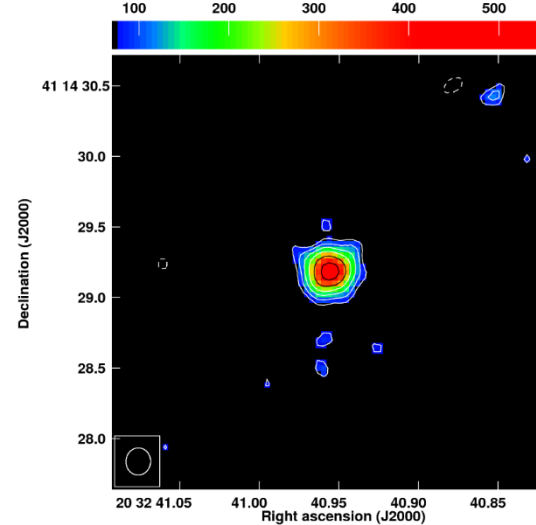
Cyg OB2 #5



Cyg OB2 #9



Cyg OB2 #12

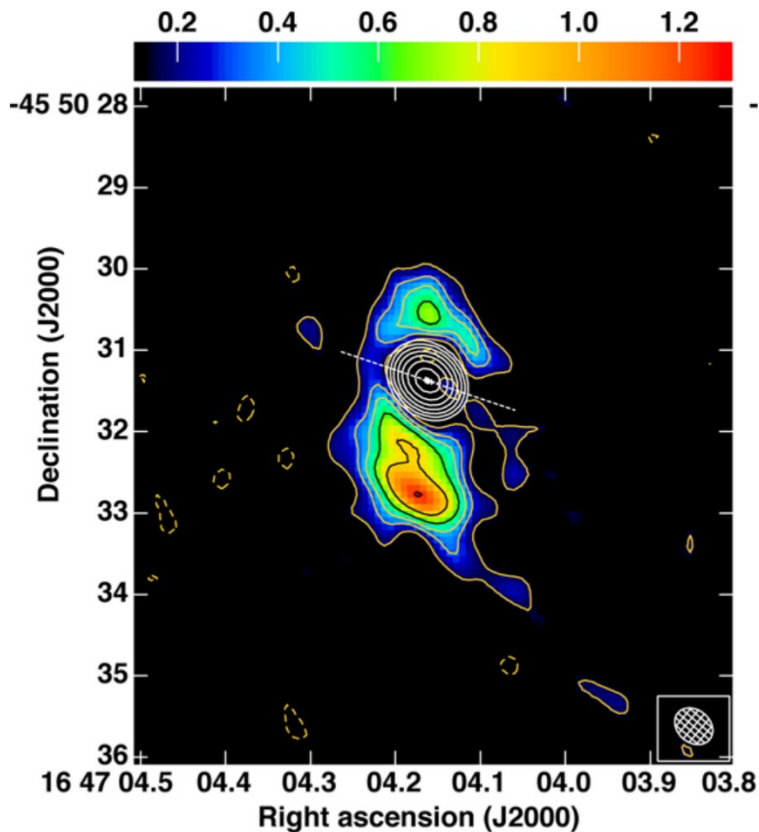


Morford et al.
2017, submitted

ALMA

Mass-loss rate $\sim 6.4 \times 10^{-5} M_{\odot}/\text{yr}$ @ 5 kpc, assuming a spherical wind

Nebula shows prior episode of significant mass loss.



Wd1-9
Supergiant B[e] star
3 mm continuum observations

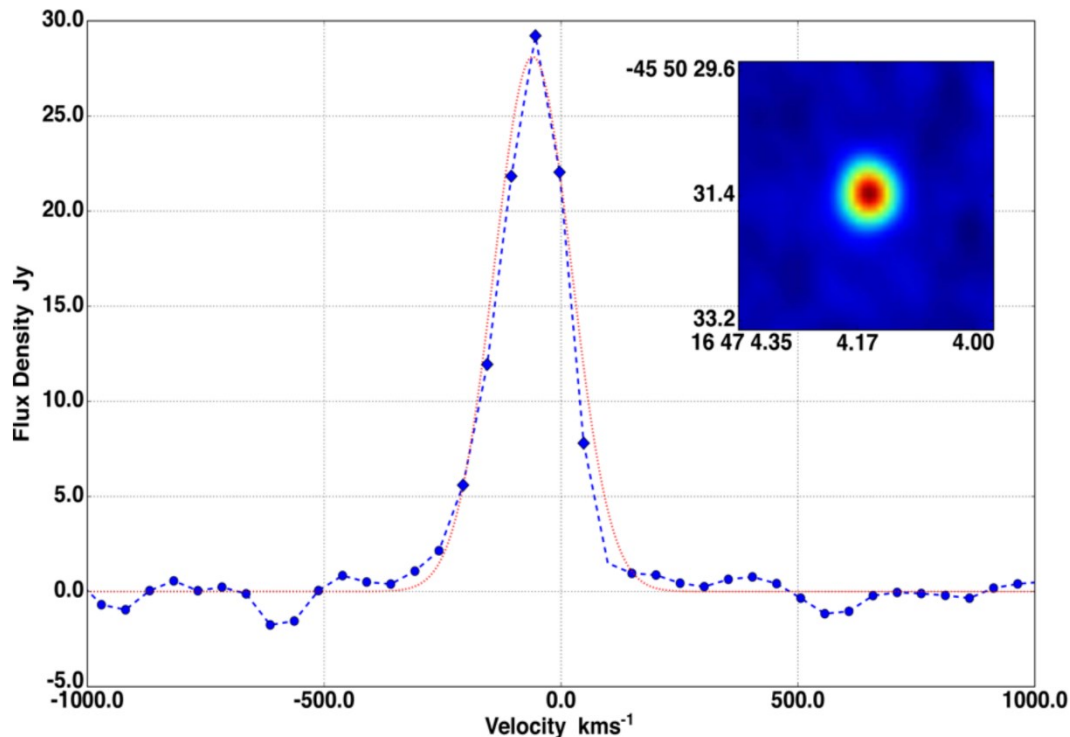
Fenech et al. 2017

ALMA

The Radio Recombination Line is formed in a rotating circumstellar disk, or in a polar outflow.

Outflow velocity of ~ 100 km/s derived from this RRL.

Wd1-9 H41 α Radio Recombination Line



Fenech et al. 2017

Surveys:

- Westerbork (WSRT) - APERTIF
 - 2π of the sky; 0.01 mJy/beam at 1.4 GHz (20 cm)

Square Kilometer Array and its precursors:

- Australian SKA Pathfinder (ASKAP)
- MeerKAT (South Africa)
 - MeerGAL: A MeerKAT high frequency Galactic Plane Survey
(PI M.A. Thompson and S. Goedhart)

Summary

- Simple relation between radio flux and mass-loss rate
- But complications:
 - Clumping/Porosity
 - Is radius dependent
 - Very probably still present in the radio formation region
 - Radio data alone cannot break the degeneracy between mass-loss rate and clumping/porosity parameters
 - Colliding-wind binaries
 - Magnetic fields
- Upgraded and new interferometers
 - ALMA: extension to mm domain
 - Radio: ideally suited for large and medium surveys (clusters)